



Research Article

Design and Characterization of 2.5D Nature-Inspired Infill Structures under Out-Plane Quasi-Static Loading Condition

Dara Ashok  and **M. V. A. Raju Bahubalendruni** 

Multi Functional Materials and Additive Manufacturing Laboratory, Department of Mechanical Engineering, National Institute of Technology Puducherry, Karaikal, Puducherry 609609, India

Correspondence should be addressed to M. V. A. Raju Bahubalendruni; bahubalindruni@gmail.com

Received 19 January 2023; Revised 21 March 2023; Accepted 22 March 2023; Published 12 April 2023

Academic Editor: Enrique Cuan-Urquiza

Copyright © 2023 Dara Ashok and M. V. A. Raju Bahubalendruni. This is an open access article distributed under the Creative Commons Attribution License, which permits unrestricted use, distribution, and reproduction in any medium, provided the original work is properly cited.

The 2.5D (2.5-dimensional) structures are acquired to enhance safety and lightweight designs with better energy absorption in the aerospace and automobile sectors. Additive manufacturing (AM), which is practical to build suitable components in industrial and transportation applications, may produce these structures more efficiently. The current study aims to improve the 2.5D infilled structures mean crush force (MCF) and energy absorption capabilities. Under compression loading, the proposed novel nature-inspired 2.5D infilled structure is compared to six existing 2.5D geometries that are inspired by nature. These structures are made of cylindrical shells that are filled with various infill configurations and maintained at a consistent volume. Photopolymer resin is used as the material for the structures, which are created using a digital light processing (DLP) method under AM technology. The characterization of the constructed models was done under compressive out-plane quasi-static stress conditions. ANSYS numerical simulations have been carried out to confirm the dependability of experimental data. The impact of supporting ribs and infill designs on crushing behaviour is thoroughly discussed. Mean crush force (MCF) and specific energy absorption (SEA) under quasi-static compression loading are provided to the proposed unique nature-inspired 2.5D infilled structure to significantly boost crushing qualities, axial collapse, and energy absorption behaviours.

1. Introduction

Cellular structures have been widely used in 2.5D structures for crashworthiness to absorb kinetic energy in engineering field crashes over the past fifty years. The 2.5D structure was fabricated without deviation in three-directional axes, but the total geometry can only be found in two-dimensional axes. Simply, the representation of three-dimensional (3D) structure in two-dimensional (2D) space is known as 2.5D representation. In today's current design, the safety and mass of the components are essential factors for contemporary design. The classic polymeric and metallic thin-walled constructions with various hierarchical designs, honeycomb and foam structure bionic tube configurations, and tremendous potentiality in lightweight and energy absorption have been utilized in various engineering applications [1, 2]. The honeycomb structures are supposed to

be used in lightweight, safe, and optimum energy utilization under quasi-static and impact loadings. These bionic tubes have several cross-sections such as a triangle, square, and circular, with numerous materials such as steel, aluminium [3], and composites [4, 5]. Due to their unique mechanical properties, honeycombs are used in aircraft wings, floor panels, rudders, jet engine shells, wind turbines, and vehicle crash boxes [6]. These structures high specific absorption energy and rigidity provide them with higher mechanical qualities, which raise their safety level when people use them.

These bionic tubes with different infill geometries are subjected axial (Out-plane) and transversal (In-plane) loaded structures with quasi-static and impact conditions. The bionic tubes with axial compressive loading can absorb higher energy with significant instability in the plastic region and unusual deformation mode. The instability of deformation in axial loading is a drawback for the structures,

and it is based on the material, infilled, and peripheral geometrical properties. When the transverse loading is subjecting, the structure bends without folding with constant large deformation.

Nature is the best place to find optimal-infilled structures with different cellular configurations formulated based on their surrounding environmental conditions [7]. With this motivation, many researchers are fascinated to adopt naturally infilled configurations with properly optimized parameters to save material and improve specific characteristics. The honeycomb structure is the most commonly used 2.5D nature-inspired infill pattern and offers extensive support with good specific strength and stiffness under quasi-static and impact loadings [8]. Due to their unique mechanical properties, honeycombs are used in aircraft wings, floor panels, rudders, jet engine shells, wind turbines, vehicle crash boxes, and so on. These bionic tubes can be fabricated with several infill geometries such as a triangle, square, and circular [9].

Bionic tubes with bamboo cross-section (BTBCs) structures inspired by bamboo's vascular microstructure of bamboo have been qualified to enhance specific energy absorption [10, 11]. In this context, Chen et al. on the absorption energy of bionic tubes with the inspiration of bamboo structures to reduce mass while increasing the peak deformation load with increasing specific absorption energy under static loading. Chen et al. studied on crashworthiness of thin-walled structures under lateral impact and bending loading condition [11, 12]. The pomelo peel-inspired structures have been developed and displayed higher energy absorption with multicell hierarchical structures [13]. The horsetail-bionic thin-walled structure (HBTS) is proposed for axial dynamic loading [14]. Gong et al. developed a thin-walled structure from the inspiration of horsetail for better energy absorption under axial dynamic loading [15]. The horsetail-based optimal design was developed using particle swarm optimization for specific energy absorption and maximum impact force [14, 16]. Several designs were developed from the inspiration of nature, such as palm/palm leaf [17], the nut shell [18], and the lotus stem [19], for enhancement of mechanical properties under quasi-static in-plane loading. The cattail-inspired structure has been incorporated in the crush box of the bumper beam to resist the impact loading and shows a significant improvement in SEA and minimal deformation [20]. Xu et al. studied the crashworthiness of bumper structures from the inspiration of cattail plant and bamboo structures that exhibited the potential advantage of energy-absorbing capabilities under impact loading [20]. Ha et al. studied the circular straight and tapered thin-walled conical corrugation bionic tubes from the inspiration from coconut trees to enhance energy absorption efficiency [21]. A hexagonal bionic tube of hierarchical bionic structures from the inspiration of a beetle has displayed excellent SEA, peak force, and crushing efficiency [22]. The Stomatopod-inspired structures displayed attractive behaviour and resisted high impacts while mineralized prey for food [23]. The concomitant calcium phosphate, calcium carbonate, carbon, and magnesium transmute, providing the impact surface [24]. The bio-

inspired Sandwich structures inspired by the turtle are designed with aluminium honeycomb attached with carbon fiber reinforced plastic (CFRP) face sheets on top and bottom to resist crashworthiness [25]. Many more biotic-inspired structures such as Oxhorn [26], Woodpecker's beak [27], Mantis shrimp [28], and Glyptodonts [29], are considered to develop the hierarchical structures for SEA under static and impact loading conditions. The versatile quality of nature-inspired infills has optimal branches to transfer the loads from the outer to the inner periphery and vice-versa.

With conventional production techniques, it is challenging to fabricate these intricate geometries. Thanks to additive manufacturing (AM) this can fabricate intricate infill structures possible with few restrictions. Because removing the support material from an enclosed body can be complicated, closed fills have often been manufactured using additive manufacturing (AM). It is well-known that removing support material from enclosed infill constructions without harming the structure during postprocessing is too tricky. One of the AM technologies uses stereolithography (SLA), or digital light processing (DLP), which is expected to produce more isotropic materials and have a smoother surface finish. The DLP 3D printer is employed for fabrication by the standards of quicker printing speed, completely dense prints, multipart builds, accuracy, and precision.

The design methodology of six existed nature-inspired 2.5D infill structures and proposed novel nature-inspired structure are discussed in Section-2. The mechanical characterization of the base material postcuring is discussed in Section-3. The experimentation on the designed structures and finite element simulation are explained with the resulted outcome under quasi-static compression loads with constant strain rate in Section-4. A comparative assessment with detailed justification is depicted with regards to the enhancement of MCF and SEA provided in Section-5. Summary of the contributions and the work's future scope in Section-6.

2. Nature Inspired Geometries and Their Fabrication

The selected structures are developed from the inspiration of nature, where the ecological system is configured to sustain under any complex loading conditions. The same structures are geometrically stochastic and difficult to formulate with unpredictable deformable and failure behaviour. Many researchers have considered examples to develop nature-inspired structures, and they are succeeded in developing and fabricating them. Those structures exhibited better mechanical performance through experimental and simulation validation. Moreover, every 2.5D structure has a different configuration in the filling space with different load-carrying capacities. The loading distribution should aim for homogeneity and manage the loading directions toward the outer nodes, so a select few have higher nodes to withstand higher loading. In each 2.5D construction, having more distribution points near the outer layer of the structure is challenging, but modifying the infill pattern procedure can achieve this.

Six nature-inspired infill patterns have been considered in the current study. These are named the turtle-inspired honeycomb infilled structures (TIHIs) [25], horsetail-inspired infilled structures (HIIs) with 10 and 12 inner branches [14], bamboo-inspired infilled structure of eight branches (BIIs), cattail-inspired infilled structures (CIIs) [20], and Palm-inspired infilled structures (PIIs) [30]. Those are considered to develop the better-infilled structures to enhance the energy absorption capability from the modern research and shown in Figure 1. The designs resemble the nature-inspired behaviour to bear the loading distribution concerning the arrangement of internal branches. The same is helping to develop the 2.5D infill configurations. The two infill designs of HIIs-10 and HIIs-12 are considered, and one better structure is considered from the set for experimentation and simulation purposes. The selection criterion is to choose the structures that display better performance over the conventional structures. The infill arrangements have various geometries, but their volumes are kept constant. The rib or infill geometry thickness is altered to keep the infill structure's volume constant.

2.1. Novel Lemon-Inspired Structure. Lemon is consisting pockets to secure the vesicles filled with its juice, extracted by squeezing. The cross-section of a lemon shows a radial layout resembling a wagon wheel, with the walls acting as the spokes, the white portion of the rind acting as the felloes, and the yellow part acting as the tire. The hub is the spongy mass in the center of the lemon. The typical lemon geometry for the current research is shown in Figure 2(a). The citrus fruit peels crimping and fruit splitting are strongly related to the thickness and hardness of the fruit peel, which are significant markers of fruit strength [31]. As a result, a thicker citrus fruit skin has a decreased risk of stretching and deforming while simultaneously having higher fracture resistance. Fruit peel toughness has a significant role in the creasing and cracking of citrus fruits. A novel lemon-inspired infill structure (NLIIs) is developed through this motivation to store the optimal energy with hierarchical geometry. The inclusion of pulp clubs strengthens the inside of the wheel. These partitions may vary in the range of 6–14 in different kinds of lemon (citrus) fruits. The inner geometry consists of a core with an average of nine links to transfer the load from the center to the outer layer. They can distribute the load uniformly throughout the geometry, as shown in Figure 2(b). The detailed view of NLIIs computer aided design (CAD) infill model is shown in Figure 2(c). The selection of an optimal number of corners can create a strong network from the core to the outside by using the shape that existed, like in the lemon, by storing the optimal energy in a longer time [32].

2.2. Specimen Fabrication. The additive manufacturing (AM) process is widely recognised for producing complicated shapes. The VAT photopolymerization technology, one of various AM techniques, is comparatively rapid, with remarkable precision, improved surface polish, and reasonable manufacturing cost. The fundamental commonality between stereolithography (SLA) and digital light processing

(DLP) is working on photopolymerization and using liquid photopolymeric materials. The polymerization approach in SLA is highly localized, nature leads to slow curing, but the DLP cures the whole layer surface at once. Therefore, all the models in this work were created on an Elegoo Mars Ultraviolet Photocuring DLP 3D Printer utilizing a liquid-based photopolymer resin. The CAD models were initially developed using CATIA V5 software, converted into a Standard Triangle Language (STL) format, further cut using Chitubox, and then produced using an Elegoo Mars DLP 3D printer. The printer features a powerful ultraviolet (UV) laser with a wavelength of 405 nm, a 125-micrometer absolute resolution, a 47-micrometer plane resolution, and a 10-micrometer layer thickness. The specimen thickness fluctuates for a constant relative density of 25% across all specimens. The exterior dimensions of all the nature-inspired 2.5D structures are 30 mm in diameter and 60 mm in height. Figures 3 and 4 display the constructed specimen and CAD models, respectively. The printed structures are postprocessed by polishing and dried with the help of isopropyl alcohol.

3. Material Properties

Tensile test samples have been fabricated and are passed for testing on Tinius Olsen equipment at a rate of 5 mm/min as per ASTM D638-14 of type-II to get the material properties after curing. The tensile specimens are fabricated in three directions, as shown in Figure 5(a) and fabricated specimens are illustrated in Figure 5(b). The uncertainties in testing are minimized by conducting five tests for the samples to characterize the photopolymer material. The tested results are consolidated and represented in Figures 5(c)–5(e) for maximum force, ultimate stresses, and modulus of elasticity, respectively. The averaged tensile test results with standard deviation have been represented in Figure 5(f) and those are used for the characterization of structures. The standard ceramic grey photopolymer resin mechanical properties are enlisted in Table 1 [33].

The deviations in the material properties are negligible due to the uncertainties in the fabrication parameters. However, the material distribution through additive manufacturing is not uniform, and often some dislocations might occur. Hence, the fabricated samples have been analyzed through the JCM-7000 scanning electron microscope (SEM) to ensure the distribution is consistent and to evaluate the printed sample's quality. All structures have been fabricated in three orientations i.e. along X, Y, and Z-directions for characterization. Due to same dissemination in all fabricated samples, only one directional fabricated sample has been considered for the illustration. The layer formation concerning the direction of printing is analyzed through SEM images at 200 μm resolution, and the fabricated direction is represented in Figure 6(a). The fabricated layers along X-axis and Y-axis as represented in Figures 6(b) and 6(c), respectively, but the visible angularity orientation of the layers is due to the sample position in the microscope. The fabrication happened in layer-by-layer formation, i.e., along the Z-axis, and the microscope images are shown in

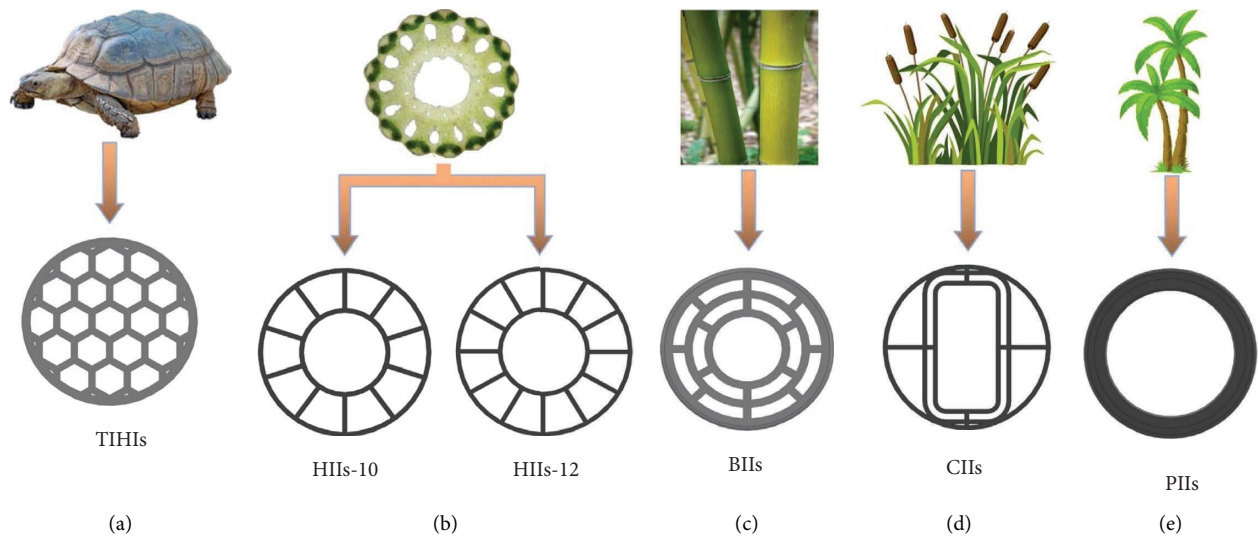


FIGURE 1: The nature-inspired infill configuration: (a) TIHIs, (b) HIIs with ten branches (HIIs-10) and HIIs with twelve branches (HIIs-12), (c) BIIs, (d) CIIs, and (e) PIIs.

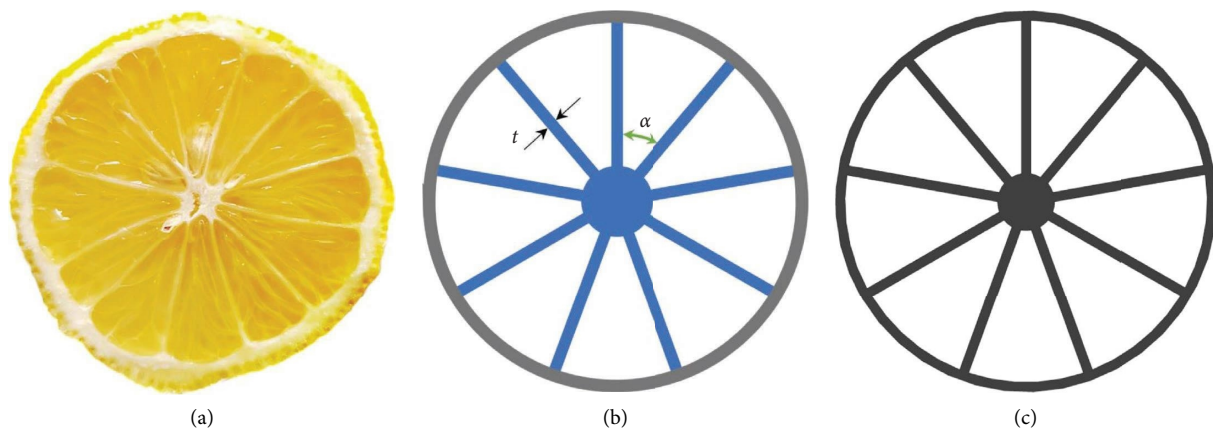


FIGURE 2: The development of NLII structure: (a) lemon (citrus) fruit structure, (b) sublayers of NLII structure and (c) CAD geometry of NLII structure.

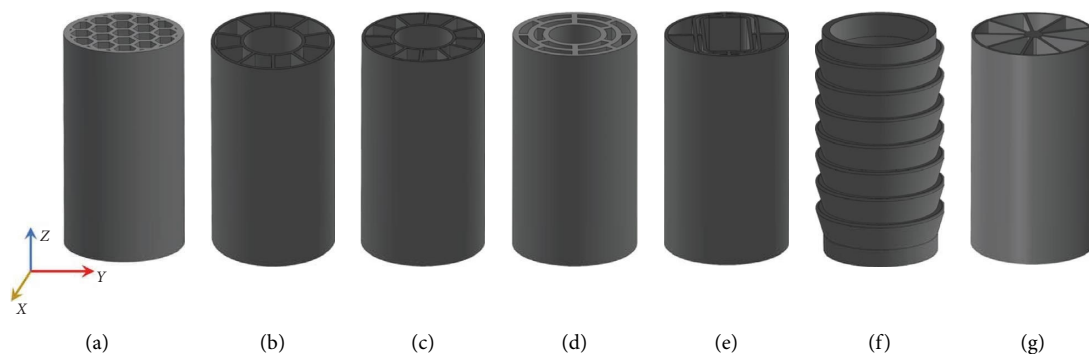


FIGURE 3: The illustration of CAD models for nature inspired infill structures: (a) TIHIs, (b) HIIs-10, (c) HIIs-12, (d) BIIs, (e) CIIs, (f) PIIs, and (g) NLII.

Figure 6(d). The sample is manufactured without printing defects and resembles the homogeneous distribution of material distribution to provide closer to isotropic behaviour, according to microscope observation.

The cracking in layer formation is the major defect while curing in printing and proper postprocessing (cleaning undissolved resin). By controlling the parameters, cracking in layer formation defects was reduced to a minimum as the

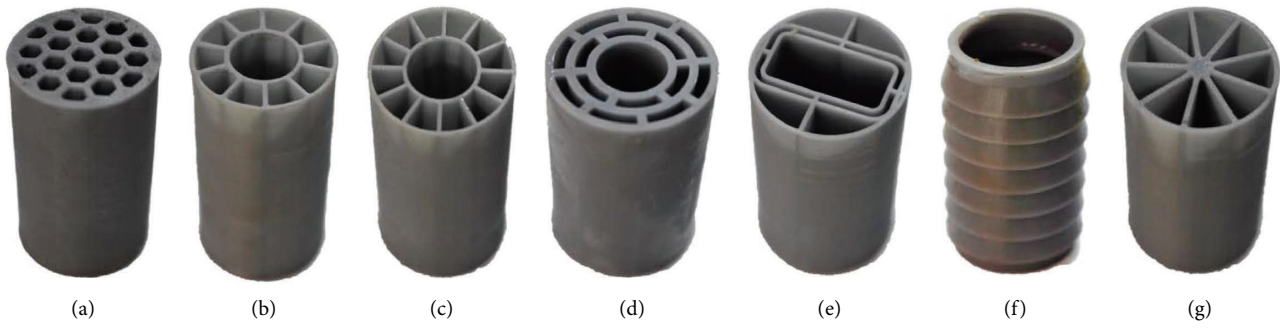


FIGURE 4: The pictorial representation of nature inspired infill structures fabricated models: (a) TIHIs, (b) HIIs-10, (c) HIIs-12, (d) BIIs, (e) CIIs, (f) PIIs, and (g) NLIIs.

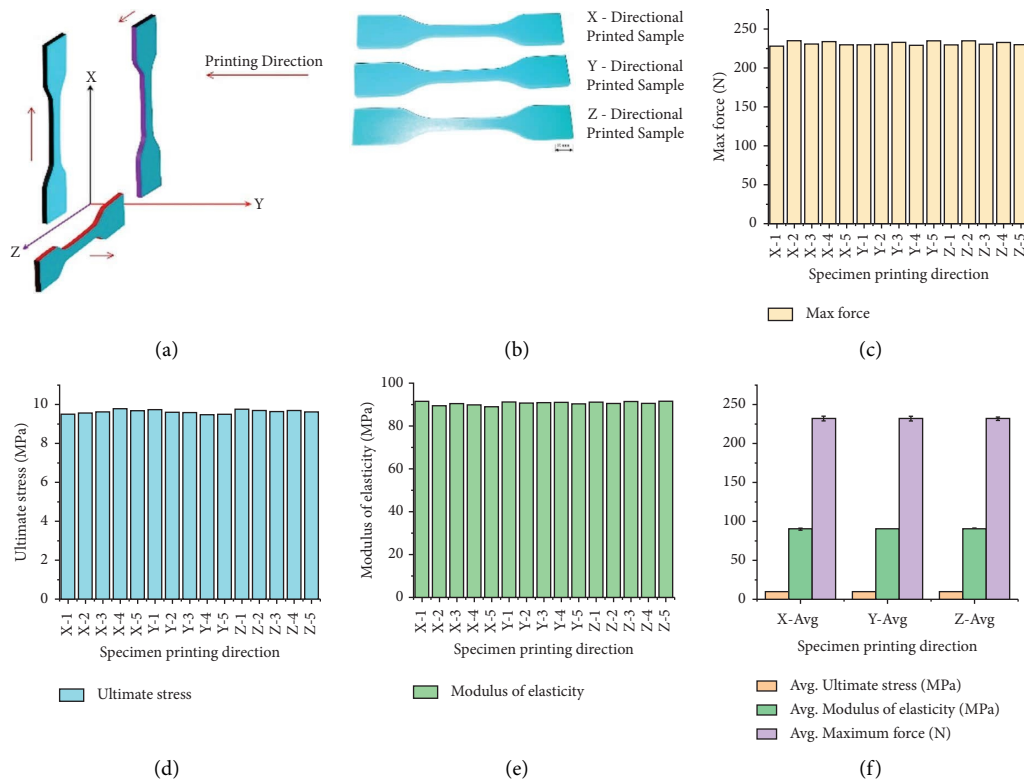


FIGURE 5: Photopolymer material characterization: (a) fabricated directions for sample preparation, (b) fabricated sample, (c–e) plots for maximum force, ultimate stresses, and modulus of elasticities for X, Y, and Z-directional fabricated samples, and (f) the average properties with standard deviation for the photopolymer material.

TABLE 1: The base material properties of the resin.

Specification	Average
Ultimate force (N)	231.67
Ultimate stress (MPa)	9.65
Youngs modulus (MPa)	90.6
Poisson's ratio	0.3167

authors were inspected in microscopic detail. The undissolved resin was soaked for optimal cleaning by isopropyl alcohol (IPA) and exposing the print to light and heated to solidify completely by attaining materials properties. This

defect exhibited minimal influence by the reliability of repetitive results.

4. Experimental and Numerical Analysis

The infill structures are tested on the Instron 8001 equipment with a maximum capacity of 100 kN under uniform loading as per D1621-16 ASTM standards [34]. The arrangement of the testing sample on the machine is located at the center of the top movable platen and allowed to move with 0.3 mm/min (0.005 m/s). This top platen moved to crush the samples by recording the stress-strain data and repeated the exact five times to verify the data repeatability

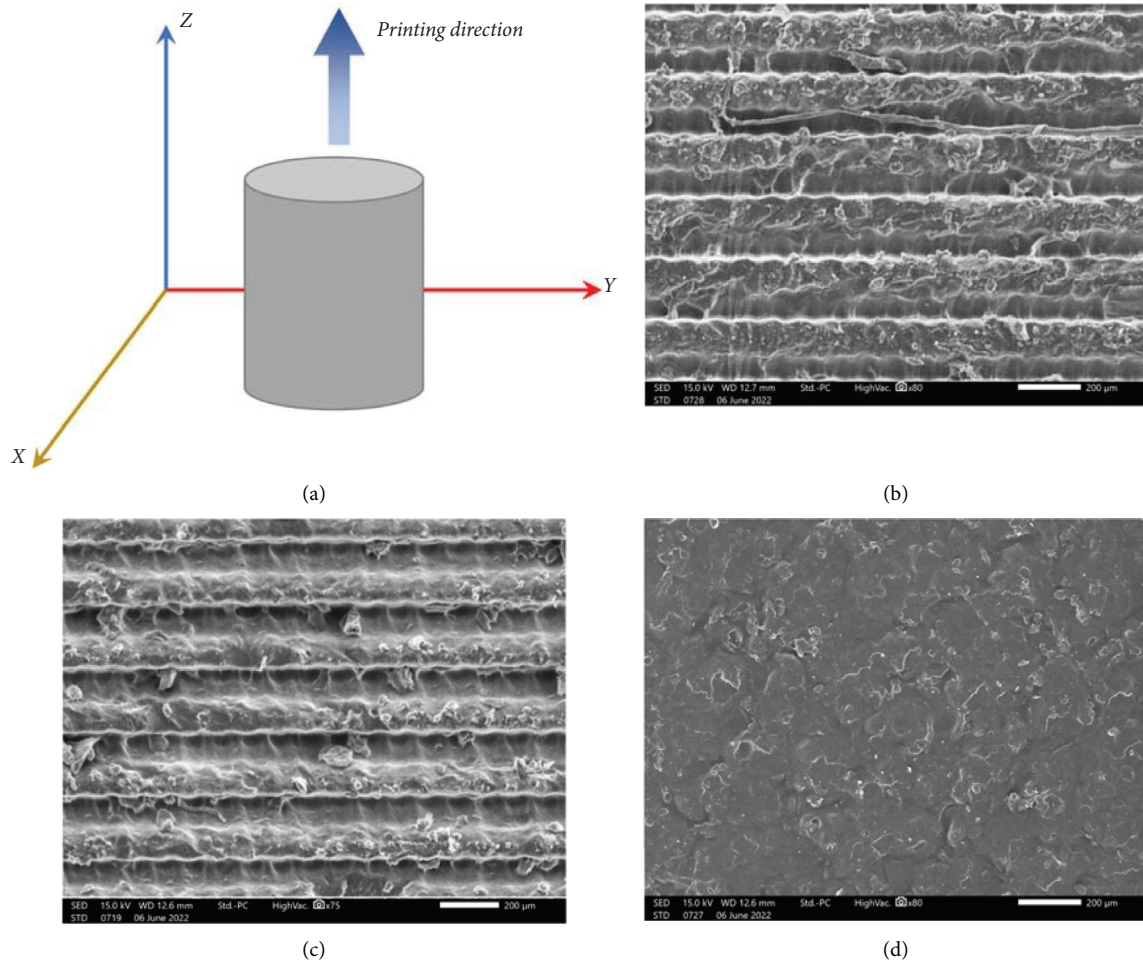


FIGURE 6: The material distribution of 2.5D infill structures through (a) printing direction and printed samples SEM images along (b) X-axis, (c) Y-axis, and (d) Z-axis.

and accuracy. The 2.5D infill structures boundary condition on the testing machine and virtual environment in ANSYS 2021 are exemplified in Figure 7. The numerical simulations have been conducted in ANSYS 2021 R2 to study the crushing behaviour of 2.5D infill structures. The modelled 2.5D infill structures are imported into the simulation as Initial Graphics Exchange Specification (IGES) file formats. The optimum mesh size has arrived at 1 mm through a mesh convergence study, and the same is maintained for the simulation. A 10-node quadratic tetrahedral element (SOLID 187) is considered for this study [35]. Parameters like geometrical and fabrication defects are neglected due to their minimal influence compared to the outcome.

5. Results and Discussion

The mechanical behaviour of existing nature-inspired infill structures and NLII structures are investigated through experimentation and numerical simulation under quasi-static compression. The resistance force obtains the stress-strain behaviour of the 2.5D infill structures concerning area and deformation. This behaviour calculates the elastic

modulus and yield point for all structures and their distribution. The structural behaviours of all samples indicate the precrushing (yield, peak load), postcrushing (plastic regime), and densification regions. After the initial peak load, the load oscillations with minor deviations are found in the postcrush stage and suddenly drop to rupture with permissible densification. Due to intrinsic geometrical arrangements, only yielding and densification are visible in the PII, HII-10 and 12, and CII structures. For HII-10 and HII-12, the HII structure offers an inner concentric circle with a 20 mm diameter, ten support ribs, and 12 ribs. The inner and outer circles absorb most of the compression force when applied, increasing the structure's peak loading capacity. Nevertheless, the break first appears on the outer surface and then loses contact with it. This resulted in the inner circle losing its capacity to carry the load. The support ribs attempted to prevent circles from buckling but failed since a rupture would occur in the middle of the structure, due to this reason for excluding the plastic region under loading in stress-strain distribution. The same type of behaviour can be observed in PII and CII structures with few plastic areas. Although it does not show peak load, the BII structure

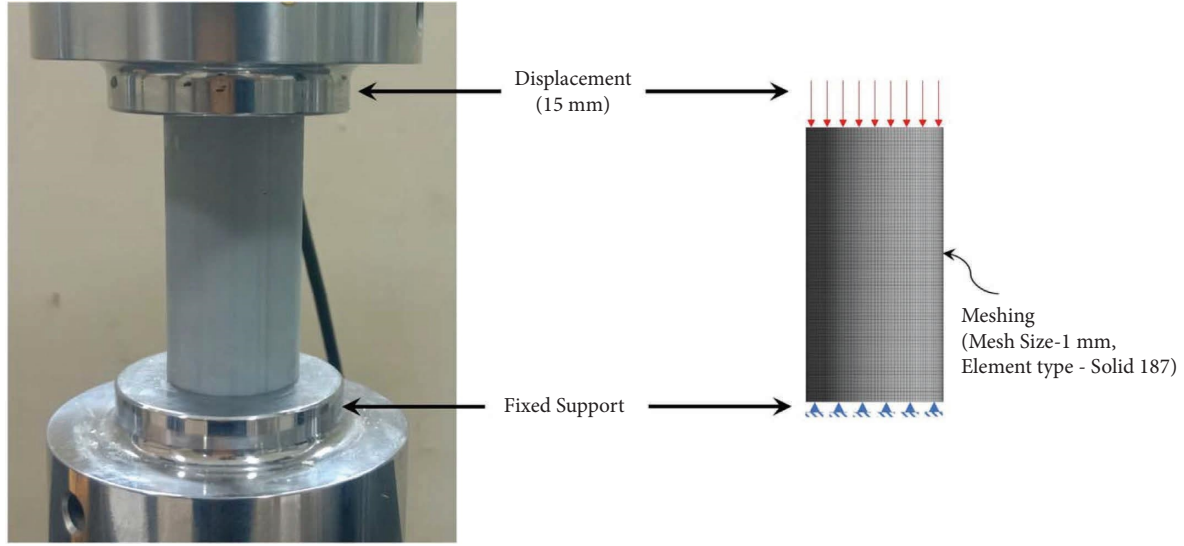


FIGURE 7: The testing sample boundary condition in the (a) machine and (b) simulation through a virtual environment.

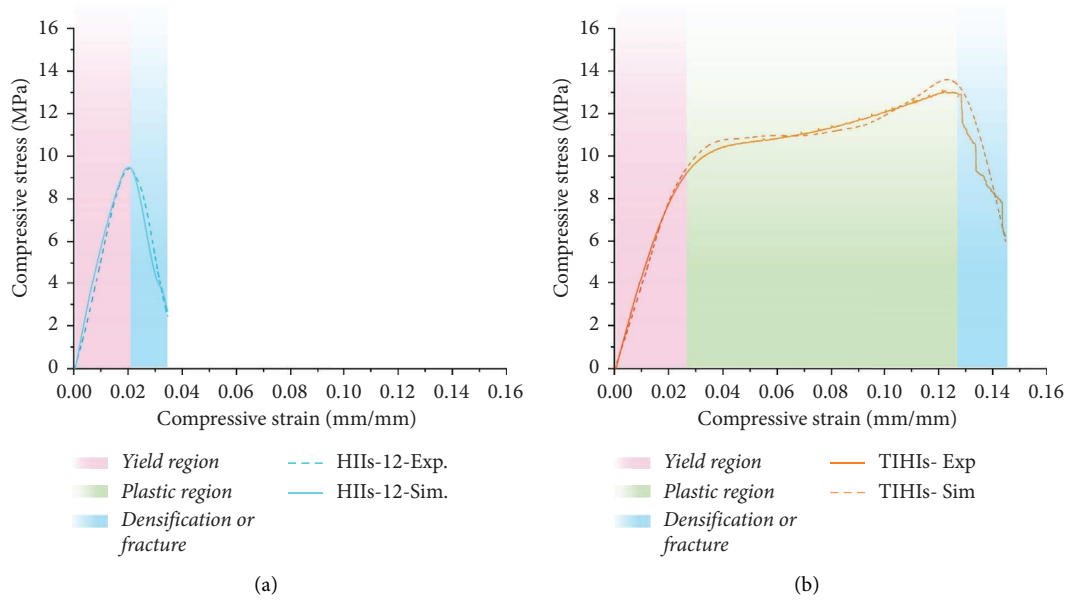


FIGURE 8: The regions in compressive stress-strain distribution for (a) HII-12 and (b) TIHI structures.

contributes little to the plastic region. Here, all sample response curves are formed with nonlinear failure with stress peaks, revealing different behaviour for all structures. The behaviour of elastic, plastic and densification regions in the stress-strain behaviour has been explained between HII-12 in Figure 8(a) and TIHI in Figure 8(b) with colour differentiation.

The main benefit of various structure infill components has been displayed in varied mean crushing force (MCF). It is referred to as the average load about the displacement of the structure, which can offer the structure's capacity for

energy absorption along the component's length, and is shown as follows:

$$MCF = \frac{EA}{\delta}, \quad (1)$$

where E = modulus of elasticity in MPa, A = cross-sectional in (m^2), and δ = crushing displacement of the structure (mm). The MCF represents the peak deceleration effect and the maximum compressive force of any structure concerning displacement. It must be low to prevent serious damage. Due to the small plastic zone, the MCF is low for all

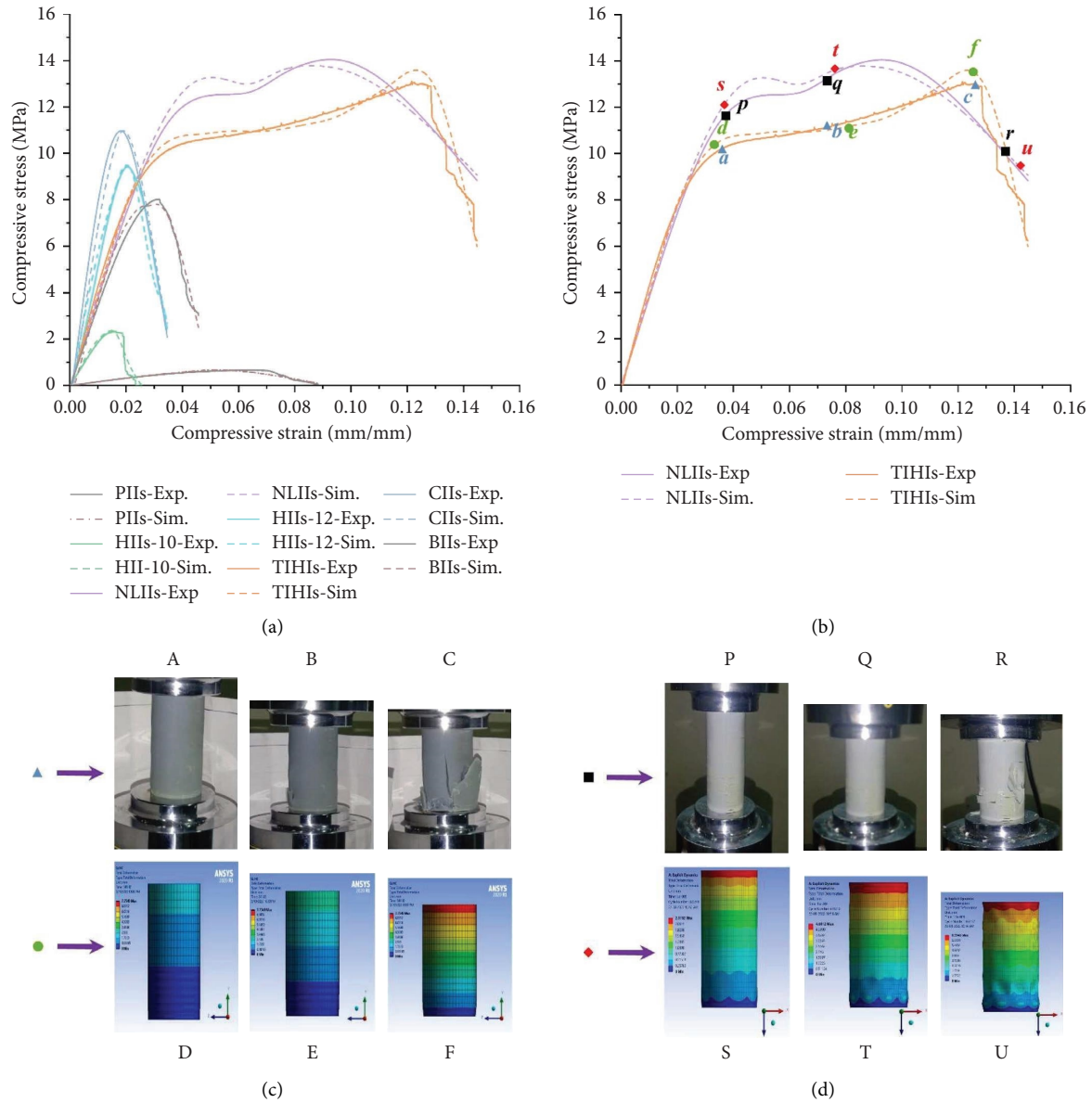


FIGURE 9: Experimental and simulation stress-strain behaviour of (a) all nature-inspired structures, (b) TIHIs and NLIIs simulation and experimental behaviour, (c) the crushing comparison of TIHI, and (d) the crushing comparison of NLIIs.

TABLE 2: The crushing parameters for nature-inspired structures.

S. no.	Sample names	Mass (gms)	Deformation (mm)		MCF (kN)		SEA (kJ/kg)	
			Exp.	Sim.	Exp.	Sim.	Exp.	Sim.
1	TIHI	13	7.3	8	9.3	9.2	1.48	1.47
2	BII	13.3	4.5	4.2	7.2	6.9	0.23	0.23
3	CII	12.8	2.4	3	6.1	5.8	0.24	0.23
4	PII	13.1	3.5	3.2	6.9	7.2	0.03	0.03
5	HII-10	12.8	2	2.3	7.3	7.3	0.03	0.03
6	HII-12	13.1	4.8	4.2	7.1	7.2	0.19	0.19
7	NLI	12.9	8.2	8.5	10.6	10.7	1.61	1.6

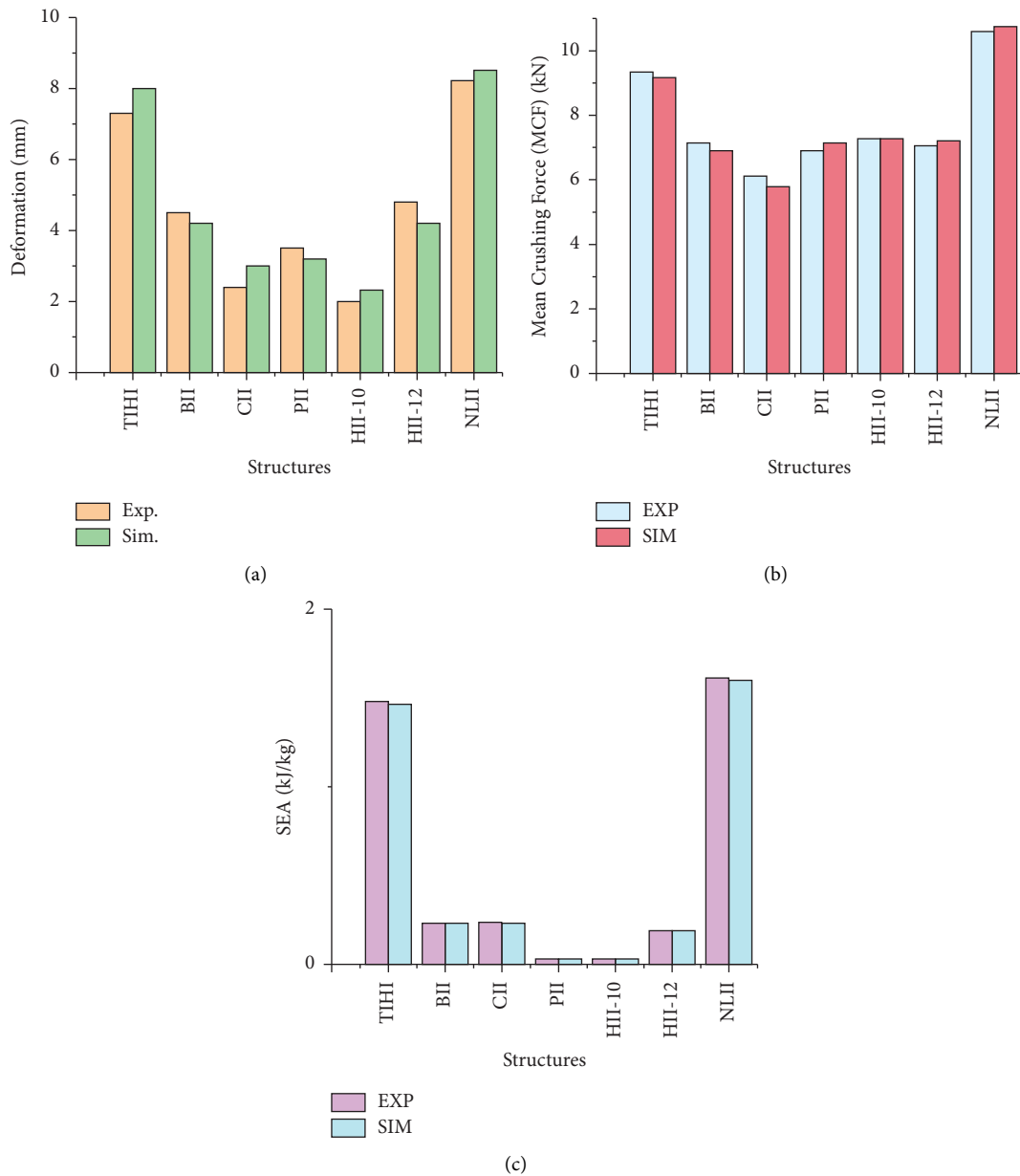


FIGURE 10: Comparison of experimentation and simulation results for all structures: (a) deformation, (b) MCF, and (c) SEA.

naturally inspired infill constructions and tents to break quickly. Due to geometrical features that also affect the MCF, the crushing displacement, or maximum displacement before the collapse, differs for each building. In comparison to the other structures, the TIHI and NLII structures had greater elastic and plastic behaviour. Regarding the actual crushing displacement, the NLII structure offers the highest MCF. The graphs in Figure 9(a) show that each building went through a slight densification stage, neared MCF, advanced into the plastic regime, and tended to collapse rapidly without further resistance. It is evident that the sublayers of the NLII geometry increased stability and had the greatest MCF. All structures MCFs vary relatively little, although those in Figure 9(b) with better plastic zones and plateau stresses, such as NLII and TIHI, are of great

importance. The sites in the stress-strain behaviour are affected by the NLII and TIHI. The NLII offers superior plastic deformation than TIHI due to how the internal structure is set up and how their supports are linked. However, under identical stress circumstances, densification and crushing failure of the structures do not utilize the same amount of energy. Among the structures, the NLII structure had the greatest MCF, whereas CIIs had a lower MCF. When compared to the TIHI (9.3 kN) structure, the NLII structure can sustain a greater compressive force of 14% (10.6 kN). The better energy absorption of NLII and TIHI 2.5D infill structures crushing mechanisms through experimentation and simulation are illustrated in Figures 9(c) and 9(d), respectively.

The amount of energy absorbed by a structure or sample with respect to mass (m) is known as the specific energy

absorption (SEA) represented in the following equation, which is calculated using the area under the stress-strain distribution.

$$SEA = \frac{EA}{m}, \quad (2)$$

where E = modulus of elasticity in MPa, and A = cross-sectional in (m^2) are and m = mass of the structure (kgs). The 2.5D infill structures, which draw inspiration from nature, are designed to absorb energy under compressive loads through structural deformation till collapse. The structure then transmits the load with less resistance, allowing for more absorption with fewer stress and strain distribution variations. The NLII structure, which improves SEA, is produced by the load transfer mechanism and the combined impact of joints with sublayers. The NLII structure outperformed the other structures in those structures in terms of energy absorption (0.21 kJ/kg). Similar behaviour is seen by TIHI, BII, CII, and HII-10 and 12, with internal branches pointing towards the outer surface, although they could withstand loading with a reduced stress distribution. Deformation is determined using the experimental and simulated stress-strain curve, and MCF and SEA are computed and presented in Table 2. As shown in Figure 10, the modelling findings and experimental data correlate well.

6. Conclusions

The current study focused on to develop the better nature-inspired 2.5D infill structure when compared to the six different types of existing nature-inspired structures for better enhancement of energy absorption applications. A novel structure inspired by the inner geometry of the lemon fruit is created to be compared to other nature-inspired infill structures. All infill structures have been modelled through CATIA software and fabricated by DLP 3D additive manufacturing approach. By using SEM analysis, the fabrication defects in every structure have been estimated, and defect-free fabrication has been made. After fabrication, all the structure has been allowed for characterization under quasi-static transverse loading as per the ASTM D1621-16 standards, while the base material mechanical properties have been characterized by tensile test with ASTM D638-14 standards. The following results have been reached based on the experimental examination and numerical modelling.

- (1) The results from the experimental and numerical simulations were observed with quite similar agreement.
- (2) The mechanical behaviour of all structures was depending on the infill geometry and topology.
- (3) The TIHI, PII, CII, HII-10, and HII-12 structures were crushed early and densified without showing considerable plastic regime; nevertheless, TIHI offers the better MCF and SEA than the other configurations.
- (4) The proposed NLII structure has proven with better enhancement of MCF by 26.5% and SEA performance by 5% over the TIHI.

- (5) The interconnectivity between the sublayers of NLII has significantly improved the MCF and SEA properties.

Data Availability

The underlying data supporting the results of the current study are included in the manuscript.

Conflicts of Interest

The authors declare that they have no conflicts of interest.

Supplementary Materials

The deformation mechanism of HII-10, HII-12, BII, CII, and PII structures under axial compressive loading are provided as supplementary file. It is possible to see the contribution of the infill of each component more clearly during the deformation mechanism. (*Supplementary Materials*)

References

- [1] Z. Yue, X. Wang, C. He et al., "Elevated shock resistance of all-metallic sandwich beams with honeycomb-supported corrugated cores," *Composites Part B: Engineering*, vol. 242, Article ID 110102, 2022.
- [2] X. Li, Z. Li, Z. Guo, Z. Mo, and J. Li, "A novel star-shaped honeycomb with enhanced energy absorption," *Composite Structures*, vol. 309, Article ID 116716, 2023.
- [3] K. Song, D. Li, C. Zhang et al., "Bio-inspired hierarchical honeycomb metastructures with superior mechanical properties," *Composite Structures*, vol. 304, Article ID 116452, 2023.
- [4] D. Ashok, V. Ramesh Mamilla, and M. V. Malikarjun, "Design and structural analysis of composite multi leaf spring," *International Journal of Emerging Trends in Engineering and Development*, vol. 5, pp. 30–37, 2012.
- [5] D. Ashok, S. Puan, R. Pradhan, and P. K. Babu, "An experimental investigation of new hybrid composite material using ramie-flax and its mechanical properties through finite element method," *Recent Trends in Mechanical Engineering*, 2020.
- [6] R. He, C. Zhao, W. Gang, Z. Zhang, and F. Li, "FEA of in-plane compression of aluminum alloy honeycomb panels," *Structures*, vol. 49, pp. 267–280, 2023.
- [7] A. Dara, M. V. A. R. Bahubalendruni, and A. J. Mertens, "Does topology optimization exist in nature?" *National Academy Science Letters*, vol. 45, no. 1, pp. 69–73, 2022.
- [8] A. Dara, A. Johnney Mertens, and M. V. A. Raju Bahubalendruni, "Characterization of penetrate and interpenetrate tessellated cellular lattice structures for energy absorption," *Proceedings of the Institution of Mechanical Engineers - Part L: Journal of Materials: Design and Applications*, vol. 237, no. 4, pp. 906–913, Article ID 146442072211297, 2022.
- [9] Z. J. Zhang, L. Huang, B. C. Li, T. Chen, Q. C. Zhang, and F. Jin, "Design of a novel multi-walled tube-reinforced aluminum foam for energy absorption," *Composite Structures*, vol. 276, Article ID 114584, 2021.
- [10] C. Chen, Z. Li, R. Mi et al., "Rapid processing of whole bamboo with exposed, aligned nanofibrils toward a high-performance structural material," *ACS Nano*, vol. 14, no. 5, pp. 5194–5202, 2020.

- [11] B. C. Chen, M. Zou, G. M. Liu, J. Song, and H. Wang, "Experimental study on energy absorption of bionic tubes inspired by bamboo structures under axial crushing," *International Journal of Impact Engineering*, vol. 115, pp. 48–57, 2018.
- [12] M. Zou, S. Xu, C. Wei, H. Wang, and Z. Liu, "A bionic method for the crashworthiness design of thin-walled structures inspired by bamboo," *Thin-Walled Structures*, vol. 101, pp. 222–230, 2016.
- [13] W. Zhang, S. Yin, T. X. Yu, and J. Xu, "Crushing resistance and energy absorption of pomelo peel inspired hierarchical honeycomb," *International Journal of Impact Engineering*, vol. 125, pp. 163–172, 2019.
- [14] Y. Xiao, H. Yin, H. Fang, and G. Wen, "Crashworthiness design of horsetail-bionic thin-walled structures under axial dynamic loading," *International Journal of Mechanics and Materials in Design*, vol. 12, no. 4, pp. 563–576, 2016.
- [15] C. Gong, Z. Bai, J. Lv, and L. Zhang, "Crashworthiness analysis of bionic thin-walled tubes inspired by the evolution laws of plant stems," *Thin-Walled Structures*, vol. 157, Article ID 107081, 2020.
- [16] H. Yin, Y. Xiao, G. Wen, Q. Qing, and X. Wu, "Crushing analysis and multiobjective optimization design for bionic thin-walled structure," *Materials & Design*, vol. 87, pp. 825–834, 2015.
- [17] E. Mahdi, D. Ochoa, A. Vaziri, and E. Eltai, "Energy absorption capability of date palm leaf fiber reinforced epoxy composites rectangular tubes," *Composite Structures*, vol. 224, Article ID 111004, 2019.
- [18] N. Xiao, M. Felhofer, S. J. Antreich et al., "Twist and lock: nutshell structures for high strength and energy absorption," *Royal Society Open Science*, vol. 8, Article ID 210399, 2021.
- [19] W. Li, K. Xu, H. Li, H. Jia, X. Liu, and J. Xie, "Energy absorption and deformation mechanism of lotus-type porous coppers in perpendicular direction," *Journal of Materials Science & Technology*, vol. 33, no. 11, pp. 1353–1361, 2017.
- [20] T. Xu, N. Liu, Z. Yu, and M. Zou, "Crashworthiness design for bionic bumper structures inspired by cattail and bamboo," *Applied Bionics and Biomechanics*, vol. 2017, Article ID 5894938, 9 pages, 2017.
- [21] N. S. Ha, G. Lu, and X. Xiang, "High energy absorption efficiency of thin-walled conical corrugation tubes mimicking coconut tree configuration," *International Journal of Mechanical Sciences*, vol. 148, pp. 409–421, 2018.
- [22] M. Zhou, D. Huang, X. Su, J. Zhong, M. F. Hassanein, and L. An, "Analysis of microstructure characteristics and mechanical properties of beetle forewings, *Allomyrina dichotoma*," *Materials Science and Engineering: C*, vol. 107, Article ID 110317, 2020.
- [23] A. B. H. Kueh and Y. Y. Siaw, "Impact resistance of bio-inspired sandwich beam with side-arched and honeycomb dual-core," *Composite Structures*, vol. 275, Article ID 114439, 2021.
- [24] J. C. Weaver, G. W. Milliron, A. Miserez et al., "The stomatopod dactyl club: a formidable damage-tolerant biological hammer," *Science*, vol. 336, no. 6086, pp. 1275–1280, 2012.
- [25] Y. Wu, Q. Liu, J. Fu, Q. Li, and D. Hui, "Dynamic crash responses of bio-inspired aluminum honeycomb sandwich structures with CFRP panels," *Composites Part B: Engineering*, vol. 121, pp. 122–133, 2017.
- [26] M. Zou, Y.-J. Yu, and R.-R. Zhang, "Simulation analysis of energy-absorption properties of thin-wall tube based on horn structure," *Journal of Jilin University (Earth Science Edition)*, vol. 45, pp. 1863–1868, 2015.
- [27] N. S. Ha, G. Lu, and X. Xiang, "Energy absorption of a bio-inspired honeycomb sandwich panel," *Journal of Materials Science*, vol. 54, no. 8, pp. 6286–6300, 2019.
- [28] J. Yang, D. Gu, K. Lin, Y. Yang, and C. Ma, "Optimization of bio-inspired bi-directionally corrugated panel impact-resistance structures: numerical simulation and selective laser melting process," *Journal of the Mechanical Behaviour of Biomedical Materials*, vol. 91, pp. 59–67, 2019.
- [29] A. Du Plessis, C. Broeckhoven, I. Yadroitsev, I. Yadroitsava, and S. G. le Roux, "Analyzing nature's protective design: the glyptodont body armor," *Journal of the Mechanical Behaviour of Biomedical Materials*, vol. 82, pp. 218–223, 2018.
- [30] Q. Liu, J. Ma, Z. He, Z. Hu, and D. Hui, "Energy absorption of bio-inspired multicell CFRP and aluminum square tubes," *Composites Part B: Engineering*, vol. 121, pp. 134–144, 2017.
- [31] J. Li and J. Chen, "Citrus fruit-cracking: causes and occurrence," *Horticultural Plant Journal*, vol. 3, no. 6, pp. 255–260, 2017.
- [32] D. Ashok, M. V. A. R. Bahubalendruni, and A. J. Mertens, "A novel nature inspired 3D open lattice structure for specific energy absorption," *Proceedings of the Institution of Mechanical Engineers - Part E: Journal of Process Mechanical Engineering*, vol. 236, Article ID 09544089221092894, 2018.
- [33] D. Ashok, M. V. A. Raju Bahubalendruni, and J. Mertens, "Numerical and experimental investigations of Novel nature inspired open lattice Cellular structures for enhanced stiffness and specific energy-gy absorption," *Materials Today Communications*, vol. 31, 2022.
- [34] Astm, *Standard Test Method for Compressive Properties of Rigid Cellular Plastics*, ASTM Stand, Pennsylvania, PA, USA, 1991.
- [35] D. Ashok, M. V. A. Raju Bahubalendruni, and J. Mertens, "Topology optimization of bench problems—stress and deformation perspective," in *Recent Advances in Manufacturing, Automation, Design and Energy Technologies*, pp. 719–729, Springer, Berlin, Germany, 2022.